Roles of Proton and Electric Field in the Electroreduction of O_2 on Pt(111) Surfaces: Results of an Ab-Initio Molecular Dynamics Study

Yixuan Wang* and Perla B. Balbuena*

Department of Chemical Engineering, Swearingen Engineering Center, University of South Carolina, Columbia, South Carolina 29208

Received: November 2, 2003; In Final Form: February 2, 2004

The electroreduction of O_2 on the Pt(111) surface is studied with Car-Parrinello molecular dynamics simulations of O_2/Pt(111), $O_2 + H^+(H_2O)_3$/Pt(111), and $O_2 + H^+(H_2O)_3 + e^-$/ Pt(111). Starting from a parallel configuration where O_2 is 3.0 Å over the Pt(111) surface along a bridge site, stepwise adsorptions of two oxygen atoms are observed, leading to a one-end chemisorption precursor (Pauling model of adsorption). The formation of the precursor has a very low barrier (0.08 eV), whereas no clear barrier was found for its decomposition. Addition of $H^+(H_2O)_3$ induces rapid formation of the proton-transfer intermediate $H^+-O_2\cdots Pt(111)$, followed by an electron transfer from the Pt slab that yields a chemisorbed precursor $H-O-O-Pt_n$, in which the hydroxyl end is considerably more separated than the oxygen end from the Pt(111) surface. Compared with the $O_2 + H^+(H_2O)_3$/Pt(111) system, the presence of an electron in $O_2 + H^+(H_2O)_3 + e^-$/ Pt(111) greatly enhances the lifetime of the proton-transfer intermediate $H^+-O-O\cdots Pt(111)$, and consequently it delays the subsequent electron transfer, which yields the formation of the one-end chemisorbed precursor $H-O-O-Pt_n$. Evolutions of the Kohn−Sham energy for the last two cases show that the formation of $H-O-O-Pt_n$ has a much higher activation barrier than its dissociation (0.4 vs 0.1 eV), indicating that the formation of chemisorbed $H-O_2$ species is the rate-determining step for the first electron transfer of the electroreduction of O_2.

1. Introduction

The oxygen molecule electroreduction (OER) takes place at the cathode of polymer−electrolyte−membrane fuel cells (PEMFC), one of the most promising future power sources and a key technology of hydrogen energy systems.[1] The slow kinetics of this reaction is one of the bottlenecks for achieving improved efficiencies in the fuel cell operation, which may lead to the rapid commercialization of these power sources. Thus, understanding the mechanisms of OER on a Pt(111) surface, currently known as one of the most active electrocatalysts of PEMFC, undoubtedly has significant implications for designing alternative cathode catalysts, with the aims of decreasing the amount of the expensive noble metal and improving the OER reaction kinetics. Therefore, many efforts have been devoted to elucidate the OER and oxygen adsorption mechanisms as discussed in a recent review.[2] Briefly, molecular oxygen is predominantly adsorbed on Pt(111) at temperatures lower than 120 K via chemical adsorption, forming chemisorbed precursor states, which may easily dissociate in the 150−500 K temperature range and mainly behave as atomic adsorption.[3] Recent Dynamic Monte Carlo simulations reproduce this phenomenon.[4] Two distinct but energetically nearly degenerate chemisorbed species have been characterized by ab-initio local spin density (LSD) calculations of the O_2/Pt(111) system,[5] by DFT calculations on cluster systems,[6] and by a variety of experimental techniques such as photoemission spectroscopy,[7−10] electron energy loss spectroscopy (EELS),[3,8] near-edge X-ray absorption fine structure spectroscopy (NEXAS),[11−13] and scanning tunneling microscopy.[14,15] One chemisorbed species is the paramagnetic superoxo O_2^- that is formed at the bridge site in a flat top−bridge−top (*t*−*b*−*t*) configuration. The other is in a nonmagnetic peroxo state (O_2^{2-}) and located at the 3-fold hollow site in a slightly canted top−hollow (fcc and hcp)−bridge (*t*−*h*−*b*) configuration.

At the operational conditions of PEMFCs where the reaction takes place at 350 K at a three-phase interface consisting of the gas phase, a water-swollen Nafion membrane, and the catalyst surface, the OER mechanisms are far more complex than at the O_2/pure Pt(111) interface, and they may depend on several factors such as interactions among hydrated protons, polymer, and water with O_2 and the rest of the intermediate species and products, in the presence of various adsorbates such as OH^- and acid groups from the polymeric membrane, as well as on the electrode potential. Experiments done under such conditions have suggested a variety of schemes for the OER in acid medium that could be generally classified into two main groups: a direct 4-electron pathway where O_2 is reduced directly to water,[16] and a series pathway including hydrogen peroxide H_2O_2 and other intermediates that will decompose or be reduced to water. Ross and Marković suggested that a series pathway via an adsorbed H_2O_2 intermediate may be operative on all Pt and Pt-based bimetallic catalysts.[17,18] In either case, it is generally postulated that the rate-determining step (rds) is the formation of adsorbed superoxide O_2^- due to the first electron transfer from the cathode.[18]

In-situ surface X-ray scattering experiments provided indirect evidence of *t*−*b*−*t* bridge adsorption of O_2 during reduction on the Pt(111) electrode surface.[19] The bridge adsorption (Yeager model) is usually believed to favor a direct four-electron reduction of O_2 on this electrode, while a considerable amount of canted adsorption (end-on adsorption,[19] Pauling model) will cause a series pathway. However, because of the difficulty of direct observation of the reduction intermediates by experimental

* Corresponding authors. E-mail: wangyi@engr.sc.edu, balbuena@engr.sc.edu.

10.1021/jp037323c CCC: $27.50
Published on Web 03/16/2004

methods, clear evidences of the OER mechanisms are still not sufficient and a number of important issues have yet to be investigated. For example, as aforementioned, it is usually accepted that the O_2 electroreduction is just thermally controlled for the O_2/Pt(111) system; nevertheless, this process is very slow in acid electrolyte solutions and it is speculated that this causes about 70% of the total loss in PEMFCs.[20] Some related questions, such as what are the roles of the solvent and proton and what causes the slow electroreduction, are addressed in this work.

First-principles-theory based computational methods, like ab-initio wave function-based electronic theory, density functional theory (DFT), plane-wave expansion DFT, and ab-initio molecular dynamics, have already become very effective tools to treat fuel cell-related electrochemical problems.[21−24] Taking into account the effect of electrode potential by matching electron affinity (EA) and ionization potential (IP) of the reactants, Anderson et al. extensively applied quantum chemistry methods to the O_2 electroreduction on Pt_2 in aqueous acid electrolytes.[23] They found that the first electron-transfer step involving proton transfer to form adsorbed O−O−H has a significantly higher energy barrier than the dissociation of O−O−H, and consequently could be considered as rds. Ab-initio molecular dynamics methods, such as Car-Parrinello molecular dynamics (CPMD),[25] have the advantage of maintaining classical molecular dynamics (MD) features without the need of an effective force field because the electron−electron and electron−nuclei interactions are obtained by solving the Schrödinger equation for the electronic structure in the Kohn−Sham (KS) DFT formulation. Thus, bond breaking and forming problems can be addressed for medium-sized systems with incorporation of environmental effects such as temperature and solvents, providing direct insights into the time evolution of reactions. Here CPMD simulations are presented for various systems: O_2/Pt(111), $O_2 + H^+(H_2O)_3$/ Pt(111), and $O_2 + H^+(H_2O)_3 + e^-$/Pt(111), to investigate the role of proton and electric field on the first electron transfer of the O_2 electroreduction.

2. Computational Details and Model Buildup

All the simulations were performed with the CPMD program, version 3.7.2.[26] CPMD implements DFT in the Kohn−Sham formulation for the calculation of the electronic structure using a plane-wave basis set, and the Car-Parrinello MD scheme[25] for the simultaneous motion of electrons and nuclei. The generalized-gradient approximation type of exchange-correlation functional (BLYP) and local spin density (LSD) theory, i.e., a spin polarized approach, were used through the present simulation to explicitly treat valence electrons. The valence electron−ion interaction was replaced by the Troullier and Martins (TM) type of norm-conserving pseudopotentials.[27] In this scheme, Pt has 10 valence electrons ($5d^96s^1$) and O has 6 ($2s^22p^4$). The wave function was expanded in plane wave basis sets with a kinetic energy cutoff of 50 Ry. Only the Γ-point was used in the Brillouin zone (BZ) sampling generated from the basis vectors of the supercell for the subsequent CPMD simulations.

The system is represented by a tetragonal supercell having dimensions of 9.58 × 8.30 × 15.81/19.22 Å, which contains a three-layer slab of Pt atoms with another five/seven equivalent layers of vacuum (in the *z*-direction perpendicular to the slab) between any two successive metal slabs; O_2 and $O_2/H_7O_3^+$, respectively, are located in this vacuum space. Previous calculations have shown that the surface relaxation has very small effects for similar systems;[28] for this reason, the Pt atoms are fixed at their bulk lattice constant (3.912 Å).[29] Each layer of slab contains twelve Pt atoms distributed in a (111) surface. Periodic boundary conditions are employed in all three spatial directions.

TABLE 1: Comparisons of Some Geometric Parameters (bond lengths: Å; bond Angle: °) Optimized with CPMD[a] and B3LYP

	CPMD[a]	B3LYP
Pt_2 (singlet)	2.345[c]	2.358[b]
Pt_2 (triplet)	2.354[c]	2.368[b]
O_2	1.254/1.248[c]	1.206[b]
H_2O	0.975 (HO), 103.0 (HOH)	0.962 (H−O), 105.1 (H−O−H)
$H^+(H_2O)_3$	1.473(H′O), 118.8(H′O′H′), 112.4(HOH)[d]	1.450(H′O), 115.9(H′O′H′), 108.6(HOH)

[a] BLYP density functional theory and spin-polarized method are employed for the CPMD simulations along with the TM pseudopotential for all atoms. [b] Pseudopotential LANL2DZ and corresponding basis set was used for Pt, and basis set 6-311++G(d,p) for H and O; [c] The data before and after the slash are using kinetic energy cutoffs of 50 and 70, respectively; [d] The atoms with and without prime belong to hydronium ion and solvent water respectively; a hydrogen bond exists between H′ and O.

To avoid excessive temperature fluctuations, the Nosé-Hoover thermostats were employed for electrons as well as for ions in the CPMD simulations. We chose 350 K as the target temperature for the ionic system to simulate the PEMFC operational condition. A fictitious electronic mass and a time step were chosen as 1100 au and 6 au (0.121 fs), respectively. The deuterium mass was used for the involved hydrogen atoms. The large fictitious electronic mass could help preserve the adiabaticity of the electronic dynamics by avoiding substantial overlap of frequency spectra stemming from the electronic and ionic dynamics and consequently preventing heating of the electronic systems. The stability of the system along the Born−Oppenheimer (BO) surface was checked by quenching the system to the BO surface for one time after 0.25 ps. No clear deviation from the BO surface was found, as evidenced by a very small reduction, in the order of 0.0002−0.0005 au, of the Kohn−Sham energy. Partial atomic charges were calculated by the method of Hirshfeld.[30]

3. Results and Discussion

To validate the TM pseudopotentials and determine the optimum kinetic energy cutoff, some isolated species were optimized using CPMD and also with B3LYP/(6-311++G(d,p) for H and O atoms, LANL2DZ for Pt) as implemented in Gaussian G98.[31] Comparisons listed in Table 1 show that the parameters from the two different methods are generally in good agreement.

3.1. O_2/Pt(111). Initially, O_2 was located in a parallel configuration, 3.0 Å above the Pt(111) surface over the 2-fold bridge site (Figure 1a). The electronic state of the total system was taken as a singlet. Snapshots of various configurations along the time evolution of this system are shown in Figure 1, which permits the visualization of the various steps of O_2 adsorption and dissociation. The path can be also monitored by time evolutions of the O1−O2 (R_{O-O}) and O−Pt(111) surface (R_{O1-S} and R_{O2-S}) distances (Figure 2a). Within the initial 0.13 ps, O1 gradually approaches the surface, while O2 tends to slightly move away from the surface, which causes rotation of the entire molecule. In the next steps, it was observed that both atoms approach the surface. According to charge population analysis, during the approach of O_2 to the Pt(111) surface, electron transfer occurs from the Pt surface to O_2, and the electron is

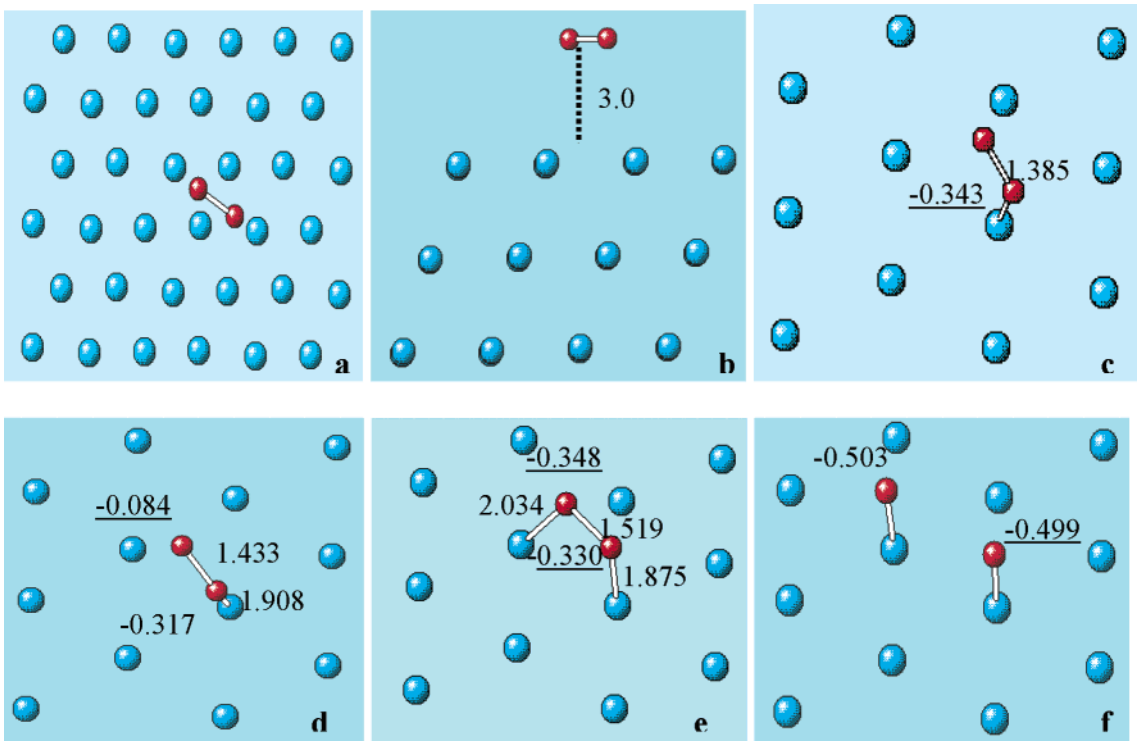

Figure 1. Snapshots of the O_2 + Pt(111) trajectory at 350 K. Only the surface layer is included in Figures (c)−(f) for clarity. The underlined data refers to the charge carried by adjacent oxygen atoms. (a) Top view of the initial configuration wherein O_2 is located parallel (3.0 Å above) to the Pt(111) surface, over the 2-fold bridge site. (b) Side view of the initial configuration. (c) One-end chemisorbed precursor at 0.24 ps, in which one oxygen is chemisorbed atop the Pt atom (at 1.85 Å) while the other oxygen is still far (2.80 Å) from the surface, and $R_{O-O} = 1.38$ Å. (d) One-end chemisorbed precursor at 0.36 ps, with distances oxygen−surface $R_{O-S} = 2.47$ and 1.91 Å, and $R_{O-O} = 1.43$ Å. (e) Top−bridge−top intermediate at 0.41 ps, with $R_{O-S} = 1.87$ and 2.03 Å and $R_{O-O} = 1.52$ Å. (f) Atop atomic adsorption at 1.16 ps.

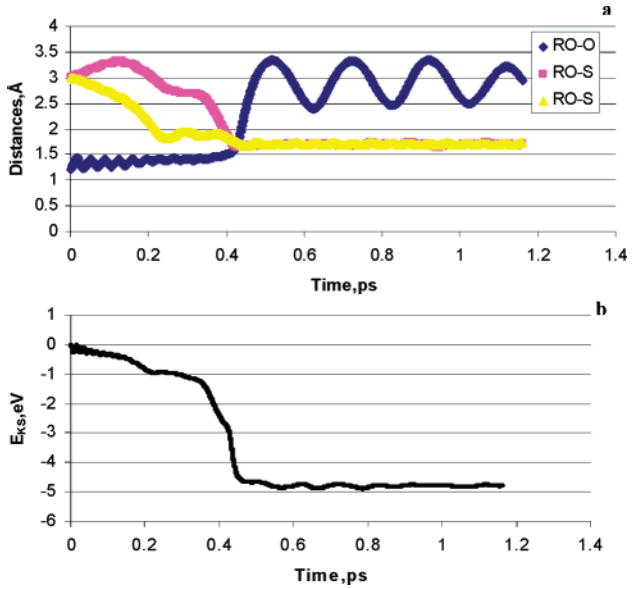

Figure 2. Time evolution of distances and energy of O_2/Pt(111). (a) O_2 bond length (R_{O-O}) and distances from oxygen to the Pt(111) surface, R_{O-S}. (b) Kohn−Sham energy.

most likely to fill in the antibonding π orbitals ($1\pi_g$).[32] Consequently, the bond length of the O_2 molecule gently becomes elongated with weaker and weaker fluctuations (Figure 2a). Meanwhile, the electronic energy (E_{KS}, Kohn−Sham energy, Figure 2b) of the entire system decreases with time. Until 0.24 ps, O1 is already quite close to the surface with a value of R_{O1-S} lower than 1.9 Å, and R_{O2-S} around 2.8 Å (Figure 1c), with an O−O distance of 1.39 Å. This end-on conformer resembles the Pauling model of adsorption,[19] and the corresponding adsorption energy predicted by the LSD method is approximately 1.0 eV. Along with the charge distribution data, the structure in Figure 1c can be identified as a superoxo chemisorption species.

Subsequently, beyond 0.24 ps, the end-on configuration (Figure 1c) gradually converts to a more stable chemisorption species (Figure 1d), a precursor of dissociation. This conversion process takes roughly 0.12 ps. During this process, the O−O bond is further extended to 1.43 Å, and R_{O1-S} and R_{O2-S} are 1.91 and 2.47 Å, respectively. This configuration is somewhat similar to the top−hollow−bridge chemisorption species extensively identified for O_2 on Pt(111) and other metal surfaces.[5,33] The precursor thence abruptly dissociates without a clear activation barrier, and the dissociation is revealed by the sudden increase of the R_{O-O} distance and by a significant drop of E_{KS}. The decrease of the electronic energy could be attributed to the atomic chemisorption of the second oxygen. The low dissociation barrier is consistent with the experimental result that adsorbed oxygen dominantly exists as atomic species on Pt(111) at high temperatures and that the dissociation of O_2 is a thermally activated process that occurs via a molecular precursor. Upon completion of O_2 dissociation ($R_{O-O} > 2$ Å), it was observed that the oxygen-to-surface distances, R_{O1-S} and R_{O2-S}, tend to be stable and the R_{O-O} distance vibrates slightly around 2.8 Å.

The above visualization suggests the following scenario as a possible mechanism for the adsorption and dissociation of a single O_2 molecule on Pt(111) at 350 K. Although initially two oxygen atoms are located equivalently above the surface, it is interesting to note that they become adsorbed in a stepwise instead of in a concerted way. Chemisorption of O1 results in the end-on chemisorbed precursor (Figure 1c), which is then converted to the more stable top−hollow−bridge type of species (Figure 1d). Such conversion has only a rather low activation

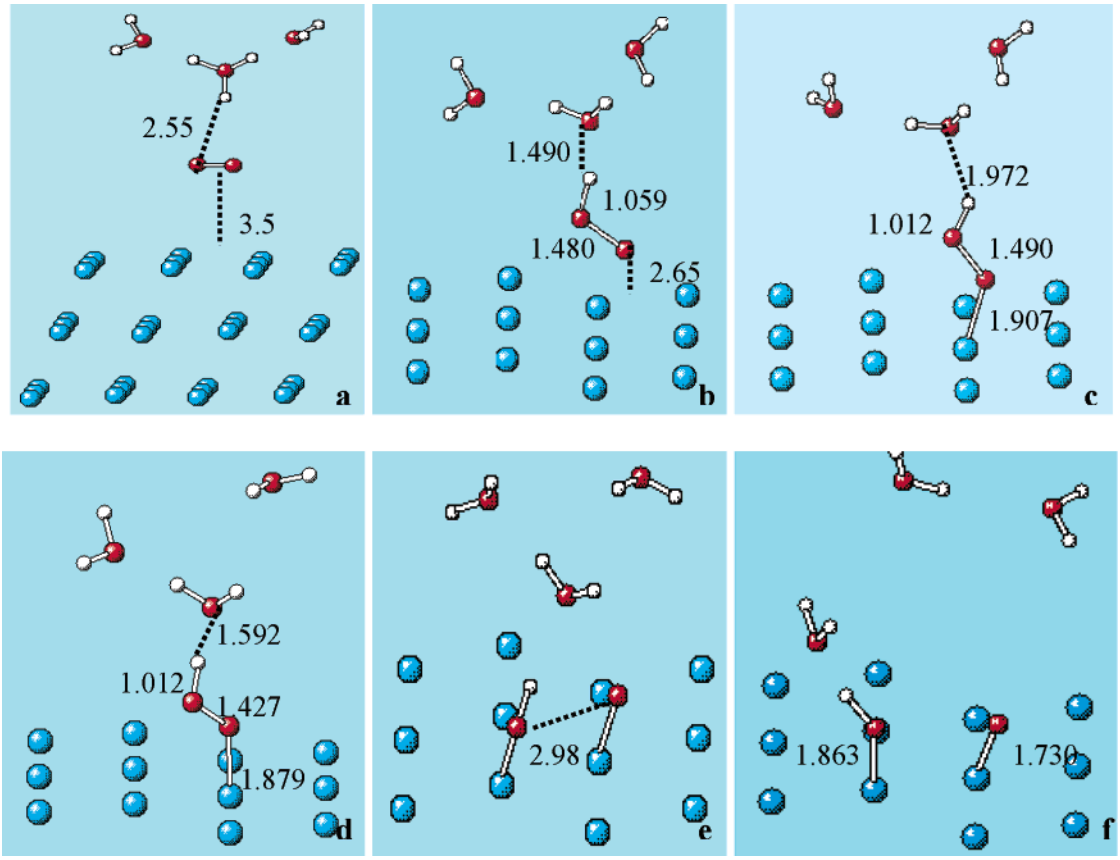

Figure 3. Snapshots of the $O_2 + H^+(H_2O)_3$/Pt(111) trajectory at 350 K. For clarity, only the surface layer is included in 3(b)−(f). (a) Side view of the initial configuration wherein O_2 is located parallel (3.5 Å above) to the Pt(111) surface, over the 2-fold bridge site, and the proton is separated from O_2 by 2.55 Å. (b) Formation of the proton-transfer intermediate $H^+-O-O\cdots Pt$ at 0.25 ps. (c) One-end chemisorbed precursor $H^+-O-O-Pt$ at 0.30 ps, wherein a strong interaction exists between the oxygen end and the Pt(111) surface, evidenced by the short distance R_{O-S} = 1.91 Å. (d) Another view of the one-end chemisorbed precursor at 0.42 ps. (e) Dissociation of the one-end chemisorbed precursor and consequent chemisorption of OH at 0.50 ps. (f) The chemisorbed hydroxyl in atop site at 0.85 ps.

barrier of 0.06 eV. No clear barrier was found for the dissociation of the molecular precursor shown in Figure 1d, which leads to atomic oxygen adsorption on Pt(111). During this dissociation, the top−bridge−top configuration shown in Figure 1e, (R_{O-O} = 1.52 Å; R_{O1-S} and $R_{O2-S} \sim$ 1.8 Å) does appear around 0.41 ps; however, its lifetime is too short to be identified as a stable chemisorbed precursor. Finally, E_{KS} converges to −4.8 eV (Figure 2, bottom). Using the experimental bond energy of 5.21 eV for O_2, these results yield an adsorption energy of 5.0 eV for a single oxygen atom, which lies in the experimental range of 2.16 to 5.20 eV.[3,34−37] It is known that adsorption energies have a coverage dependence such that lower coverages usually lead to higher binding energies due to lower O−O repulsive interactions.[37] Thus, the present relatively high adsorption energy may be related to the low coverage.

The ab-initio molecular dynamics simulation of O_2 on Pt(111) at 350 K verifies some common knowledge such as thermally activated molecular dissociation and consequent preference of atomic adsorption. It also provides new insights into its adsorption and dissociation, such as that a relatively stable one-end chemisorbed precursor results from stepwise adsorptions of two oxygen atoms, and that the well identified (at low temperatures) top−bridge−top chemisorbed intermediate has a very short lifetime. The oxygen adsorption has also been investigated with another initial configuration, a perpendicular configuration, where the molecular axis of O_2 is perpendicular to Pt(111) and a distance of 3.0 Å between the closest oxygen and the surface. O_2 chemisorption and dissociation were not observed in this case, indicating that adsorption of O_2 on Pt(111) strongly depends on the initial configuration, this aspect will be discussed separately in a future publication.

3.2. $O_2 + H^+(H_2O)_3$/Pt(111). To approximate the condition of hydrated protons present in the water-swollen Nafion membrane of PEMFCs, a well-hydrated proton $H^+(H_2O)_3$ was introduced into the supercell and the effect of proton and water on the adsorption and electroreduction of O_2 was examined. This part of the study also allows investigating the role of proton transfer and its correlation with electron transfer. Simulations on positively charged species were performed with the corresponding negative charge distributed uniformly in the cell.[38]

In the initial configuration (Figure 3a), O_2 is located as in Figure 1a, but 0.5 Å farther from the Pt(111) surface, and the proton of $H^+(H_2O)_3$ is separated from O_2 by 2.55 Å. From the time evolution of the distances shown in Figure 5a, it was observed that within the initial 0.25 ps, the hydrated proton gradually migrates toward O_2 and at approximately 0.12 ps the accompanying water molecules begin to separate, bringing about a proton-transfer intermediate shown in Figure 3b ($H^+-O-O\cdots Pt(111)$), where R_{H-O} (distance between proton and oxygen atom of O_2) and R_{H-O_W} (distance between proton and oxygen atom of water) have values of 1.06 and 1.48 Å, respectively. During the course of this event, the bond length of O_2 elongates (to ∼1.48 Å) while fluctuating (Figure 5b) because of the proton effect and the possible weak interaction between H^+-O_2 and the Pt(111) surface, since the two O atoms are still far from the surface ($R_{HO-S} \sim$ 3.5 Å; $R_{O-S} \sim$ 2.7 Å) and the electron transfer

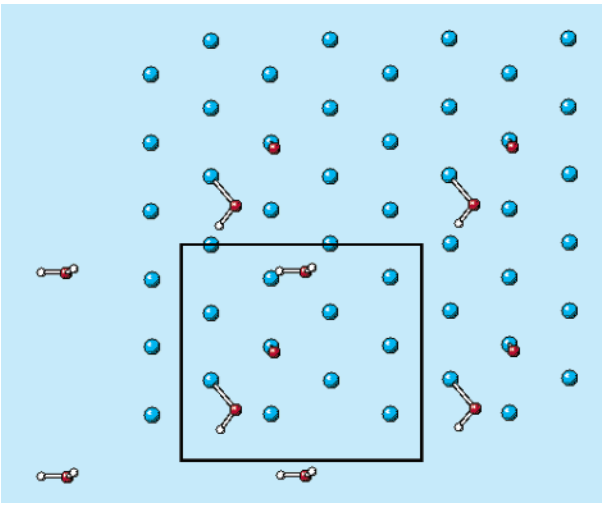

Figure 4. Top view of the surface layer of absorbed oxygen, hydroxyl, and H_2O species at 1.45 ps. The supercell (boundary shown by the solid line) and its partial neighbor periodic images are shown. The distances from the adsorbed hydroxyl oxygen to its nearest three Pt atoms are 2.01, 2.17, and 2.53 Å.

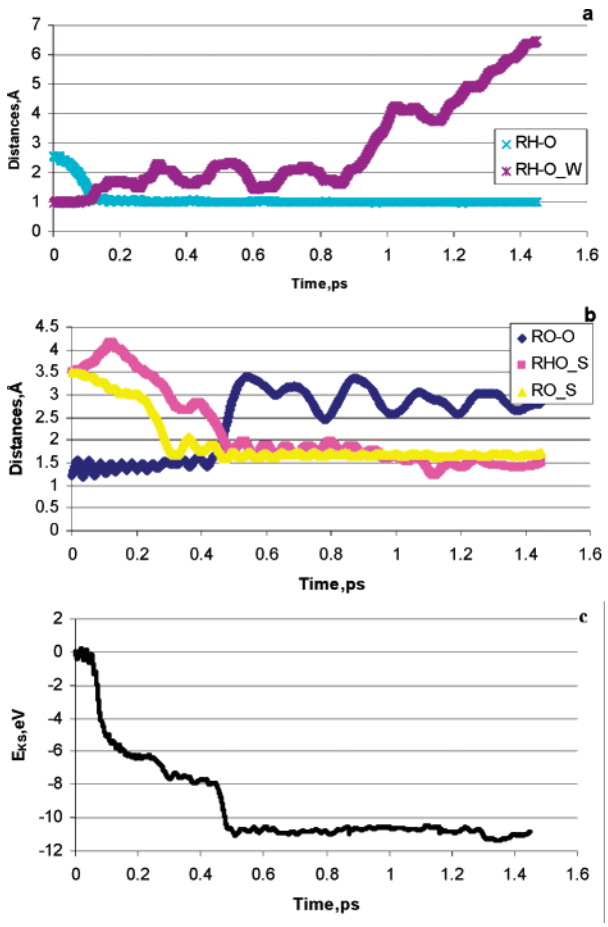

Figure 5. Time evolutions of distances and energy of the $O_2 + H^+(H_2O)_3$/Pt(111) system. (a) Distances from the proton of H_3O^+ to O_2 (R_{H-O}) and to the hydronium oxygen (R_{H-O-W}). (b) O_2 bond length (R_{O-O}) and distances from oxygen and hydroxyl oxygen to the Pt(111) surface, R_{O-S} and R_{HO-S}. (c) Kohn−Sham energy.

from Pt(111) is not expected to take place at the conditions in Figure 3b.

Similarly to the case of O_2/Pt(111), the two oxygen atoms in the proton-transfer complex shown in Figure 3b are adsorbed on the Pt(111) surface one after another, the hydroxyl radical later than the oxygen atom. Until 0.3 ps, the distances (R_{HO-S} and R_{O-S}) from these species to the Pt(111) surface are approximately 2.9 and 1.7 Å, respectively, indicating the formation of the one-end chemisorption species as shown in Figure 3c. In the following 0.13 ps, R_{O-O} and R_{O-S} (Figure 5) gently vibrate around 1.5 and 1.8 Å, respectively. As the hydroxyl oxygen atom continuously approaches the surface, the species shown in Figure 3c is converted to the more stable chemisorption species shown in Figure 3d, a chemisorbed precursor for O_2 dissociation. According to population analysis, the electron is clearly transferred from the Pt slab to the proton-transfer intermediates in the configurations 3c and 3d. A similar phenomenon had been detected for alike systems in small Pt clusters.[39] The proton-transfer intermediate ($H^+-O-O\cdots Pt_n$) leads to a higher adsorption energy of H^+-O-O than that of O_2 on Pt(111) (~2.3 vs 1.0 eV).

After formation of the chemisorbed precursor (Figure 3d) at approximately 0.42 ps, the O−O bond begins to rapidly dissociate (Figure 5b), which is reflected by the sudden separation of the two O atoms, and further approach of O and OH to the Pt(111) surface (Figure 3e). Over the following period, the R_{O-O} distance fluctuates around 3.0 Å, and R_{O-S} shows a slight oscillation around 1.7 Å. Passing through a short steep decrease, the distance from the hydroxyl oxygen to the Pt(111) surface (R_{HO-S}) vibrates around 1.8 Å, a slightly higher value than that of R_{O-S}. This indicates that the hydroxyl is chemically adsorbed at a top site (Figure 3f). Until 0.85 ps, a hydrogen bond exists between the chemisorbed hydroxyl and a water molecule, which is revealed by the vibration around 1.8 Å of the R_{H-O_W} distance (Figure 5a). The hydrogen bond determined a strong preference for hydroxyl adsorption on a top site, versus adsorption in hollow or bridge sites. This is consistent with the reported finding for high coverages of OH_{ads} on Pt(111) where H-bond formation between adjacent adsorbed OH groups enhances their atop adsorption.[40] After the cleavage of the hydrogen bond beyond 0.85 ps, R_{HO-S} decreases and fluctuates around 1.5 Å, which implies that OH is adsorbed on a bridge site. A snapshot displaying partial neighbor periodic images shown in Figure 4 illustrates the surface layer including absorbed oxygen, hydroxyl, and H_2O species from the simulation at 1.45 ps. The distances from the hydroxyl oxygen to the nearest three Pt atoms are 2.011, 2.166, and 2.525 Å, respectively. Therefore, under these conditions, adsorption of OH is most likely to be classified as a bridge adsorption despite the slightly different distances between OH and each of its two closest Pt neighbors.

In contrast to the case of O_2/Pt(111), a close inspection of E_{KS} indicates that the formation of the most stable chemisorbed species (Figure 3d) has a significant barrier of approximately 0.4 eV, whereas the barrier of its decomposition is only about 0.1 eV. This result is in qualitative agreement with the findings of Anderson's group.[23] The CPMD trajectory of $O_2 + H^+(H_2O)_3$/Pt(111) shows that proton transfer occurs very early to form a proton-transfer intermediate $H^+-O-O\cdots$Pt(111), which has much higher electron affinity than O_2 due to the proton field, and consequently induces the subsequent electron transfer from the Pt slab. As a result of such electron transfer, a one-end chemisorbed precursor $H^+-O^{\delta-}-O^{\delta-}-Pt_n$ is generated. The hydroxyl species is still beyond 2.5 Å from the Pt(111) surface when the O_2 dissociation begins in the $H^+-O^{\delta-}-O^{\delta-}-Pt_n$ complex; it approaches the surface during the dissociation process and eventually is chemisorbed on the surface.

Overall, the proton is involved in the dissociation of O_2, and significantly increases the activation barrier for the formation

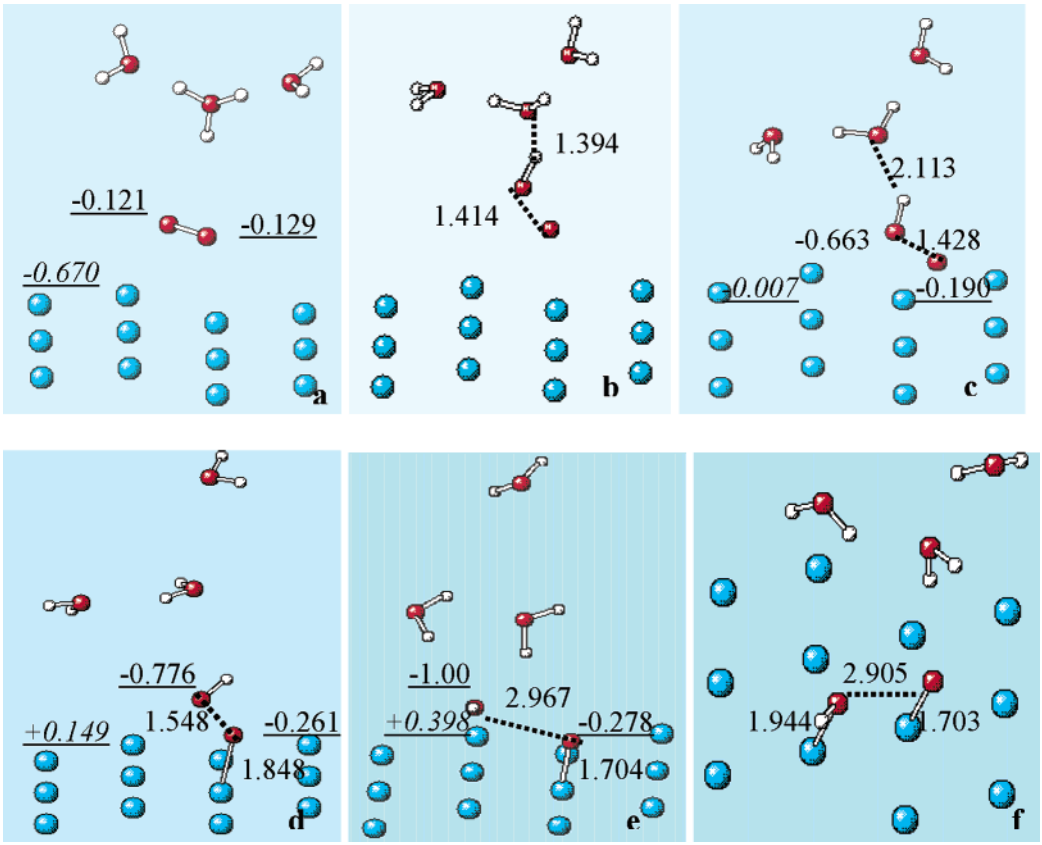

Figure 6. Snapshots of the $O_2 + H^+(H_2O)_3 + e^-$/Pt(111) system at 350 K. For clarity, only the surface layer is included. The underlined data refers to the charge carried by oxygen atoms, but the values (in italics) shown on the surface are cumulative charges borne by the Pt slab. (a) Side view of the initial configuration. (b) Proton-transfer intermediate H−O−O generated at 0.15 ps. (c) Proton-transfer intermediate H−O−O at 0.44 ps. (d) One-end chemisorbed precursor H−O−O−Pt_n (adsorbed) at 0.53 ps. (e) H−O−O−Pt_n dissociation into H−O and O (adsorbed) at 0.73 ps. (f) Atop atomic adsorption at 0.89 ps.

of the one-end chemisorbed precursor $H^+-O^{\delta-}-O^{\delta-}-Pt_n$ as compared with the case of O_2/Pt(111). Likewise, a rather low barrier for the dissociation of the precursor is predicted for this case.

3.3. $O_2 + H^+(H_2O)_3 + e^-$/Pt(111). In an attempt to incorporate the effect of an electric field, the Pt slab was charged by introducing a negative charge to the supercell. Population analysis confirms that the slab carries the negative charge. Considering the fact that a strong electric field exists across the double layer as a consequence of the surface charge, the proposed charged model is used as an approximation for studying the effect of the electrode overpotential on electrochemical reactions. The electronic state of the overall system is a doublet.

The overall sequence of essential events is summarized in Figure 6. Similarly to the previous case, H_3O^+ rapidly approaches O_2 to form the proton-transfer intermediate ($H^+-O-O\cdots$Pt(111), Figure 6b) within 0.15 ps, which is evidenced by a drastic decrease of the R_{H-O} distance and a slow increase of R_{H-O-W}, shown in Figure 8a. Shortly after this, the H−O bond of the hydronium ion is broken, yielding water while the proton transfer to the O_2 molecule is almost completed at this step. Compared with the previous case of $O_2 + H^+(H_2O)_3$/Pt(111), the proton-transfer complex exists for much longer times, until 0.48 ps. During the formation of the proton-transfer intermediate, although the oxygen atoms of O_2 gradually approach the metal surface, the shortest R_{O-S} distance is still further than 2.6 Å, and the R_{HO-S} distance is even longer. Hence, no clear chemisorption could be expected for $H^+-O-O\cdots$Pt(111) at this stage. Over the next 0.05 ps, the O atoms rapidly move toward the Pt(111) surface, this process is accompanied by a sudden decrease of E_{KS} (Figure 8c), indicating that a one-end chemisorbed species begins to be generated. As shown in Figure 8 by the time evolutions of the R_{O-S} and R_{HO-S} distances as well as that of E_{KS}, the one-end chemisorbed species is converted to a stronger chemisorbed species with slightly higher adsorption energy, by increasing R_{O-S} and decreasing R_{HO-S}, within approximately 0.1 ps, whereas the R_{O-O} bond length vibrates around 1.5 Å. Thus, after the one-end chemisorption precursor was well generated at 0.6 ps (Figure 6d), the H−O−O−Pt(111) complex begins to homolytically decompose into adsorbed hydroxyl and adsorbed O (Figure 6e); this process is well illustrated by the sudden increase of R_{O-O} (Figure 8b).

During the following 0.15 ps, the R_{HO-S} distance monotonically decreases until the complete decomposition of H−O−O−Pt(111) takes place at about 0.80 ps, while R_{O-O} reaches about 3.0 Å (Figure 6e). This indicates that the decomposition of H−O−O and the chemisorption of hydroxyl do not occur simultaneously; instead the decomposition is followed by the OH adsorption. Thus, it is the decomposition that induces the chemisorption of the hydroxyl species. The R_{HO-S} distance then decreases rapidly, and it vibrates around 1.8 Å for some time, and around 1.65 Å thereafter, showing that HO is first absorbed atop (Figures 6e and f) and then diffuses to a bridge site (Figure 7a). Beyond 1.4 ps, the R_{HO-S} distance further decreases to approximately 1.2 Å. To illustrate the OH adsorption, two snapshots of the surface layer containing absorbed O, OH, and H_2O species at 1.02 and 1.71 ps, respectively, are shown in Figure 7. In Figure 7a, the distances from the hydroxyl oxygen to the nearest three Pt atoms are 1.95, 2.16, and 2.37 Å,

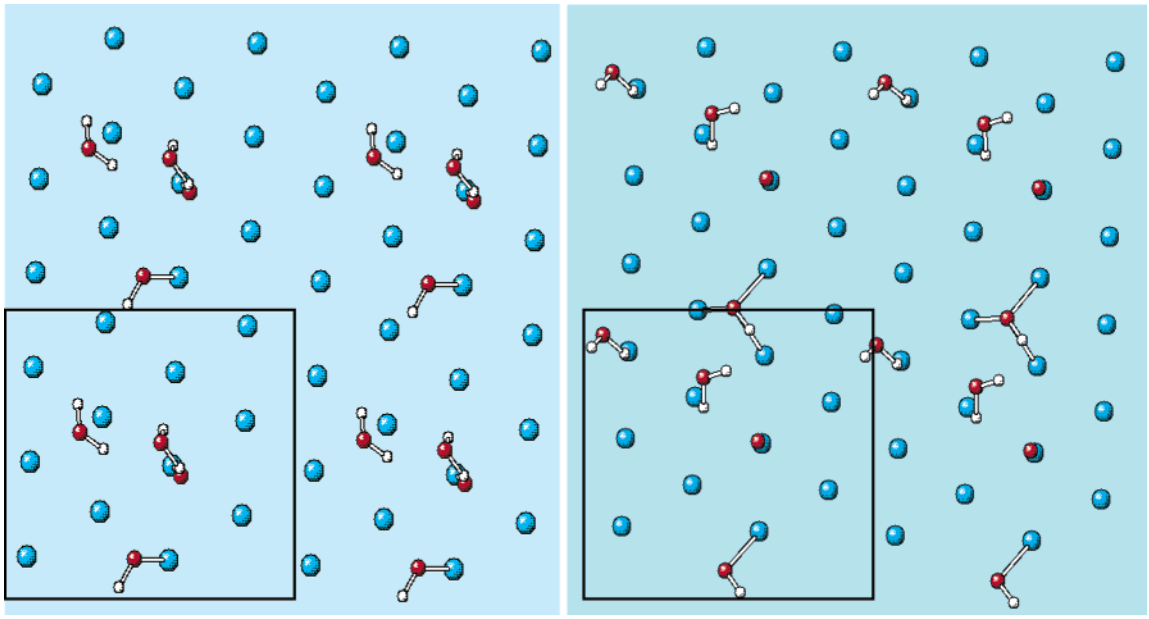

Figure 7. Snapshots of the surface layer of absorbed oxygen, hydroxyl, and H_2O species. The supercell (boundary shown by the solid line) and its partial neighbor periodic images are shown. (a) At 1.02 ps. The distances from the hydroxyl oxygen to the nearest three Pt atoms are 1.95, 2.16, and 2.37 Å. (b) At 1.71 ps. The distances are 1.81, 1.97, and 2.05 Å.

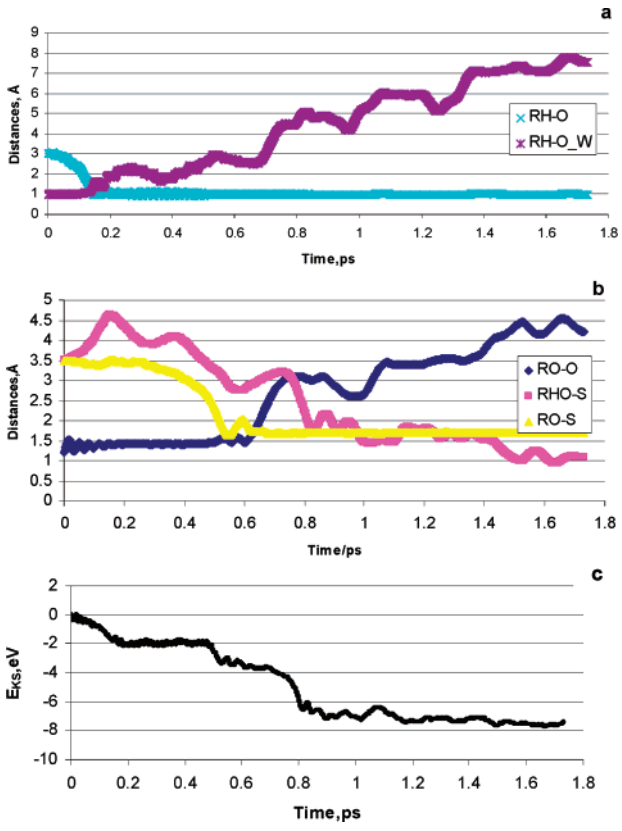

Figure 8. Time evolutions of distances and energy of the $O_2 + H^+(H_2O)_3 + e^-$/Pt(111) system. (a) Distances from the proton of H_3O^+ to O_2 (R_{H-O}) and to the hydronium oxygen, (R_{H-O-W}). (b) O_2 bond length (R_{O-O}) and distances from oxygen and hydroxyl oxygen to the Pt(111) surface, R_{O-S} and R_{HO-S}. (c) Kohn−Sham energy.

respectively, while they are 1.81, 1.97, and 2.05 Å in Figure 7b. Thus, in both cases the adsorbed OH is strongly interacting with one Pt atom; however, there is a tendency toward OH adsorption on the bridge and even hollow sites, as found by others.[40,41]

According to Figure 8c, the formation of the one-end chemisorption precursor H−O−O−Pt_n has an energy barrier of approximately 0.4 eV and its dissociation has only a small barrier of less than 0.1 eV, values that are extremely close to those of the previous case. Thus, it is most likely that the presence of the added electron just extends the lifetime of the proton-transfer intermediate, H−O−O···Pt_n; however, it has little effect on the energetics of the formation and subsequent dissociation of the chemisorption precursor.

To further discuss the correlation between electron and proton transfers, we computed net charges defined as the sum of the atomic charges for a given system. The time evolution of net charges is displayed in Figure 9 for the metal slab and proton-transfer intermediate O−O−H. Initially, the charge distribution in the slab yields a net charge per layer (not shown) of −0.08e (top layer, surface), +0.56e (middle) and −0.23e (bottom) for the uncharged system, whereas the respective values for the negatively charged system are −0.26e, +0.12e, and −0.53e; the resultant initial net charge for the slab is 0.25e for the uncharged and −0.67e for the charged system (see inset), whereas the O−O−H group initially carries an almost identical net charge (+0.6e) for the two cases. The slope of the curves in Figure 9 provides an estimate of the instantaneous rate of charge transfer in each system. For example, Figure 9 shows that a small amount of charge (∼0.16e) was transferred from the metal slab to the O_2 molecule with the formation of the hydrated proton-transfer-intermediate within the first 0.10 ps. Shortly after this, the charged metal slab transfers considerably more electrons than the uncharged one, e.g., 0.60e vs 0.4e at 0.15 ps. This would indicate that the electron would be more readily transferred from the negatively charged slab; however, subsequent relaxation of the proton-transfer intermediate including its dehydration requires a much longer time for acceptance of further charge, probably due to the stronger electrostatic attraction between the charged slab and the intermediate, whereas the interaction is much weaker for the uncharged case. During the relaxation of the intermediate for the charged slab, there is no further electron transfer between the slab and the intermediate (Figure 9, flat region). The following charge transfer (∼0.3e) causes the formation of the chemisorbed precursor. In both cases, as shown in Figures 5c and 8c, there exist isomerizations between chemisorbed species, leading to

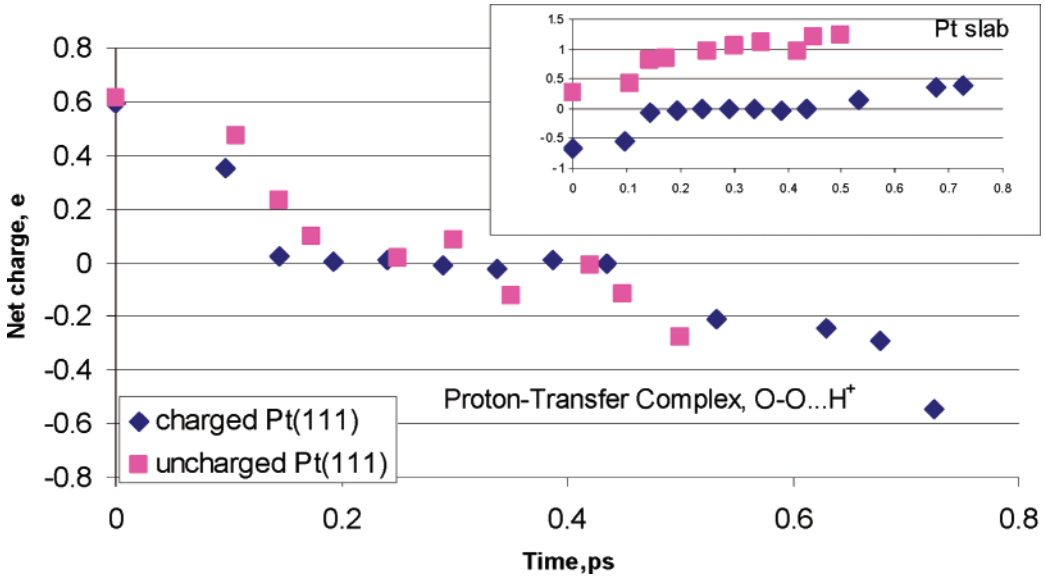

Figure 9. Evolutions of the net atomic charges (defined as the sum of the atomic charges) of the metal slab (inset) and those of the proton-transfer complex, for the negatively charged (black diamond) and uncharged (purple square) systems.

the most stable chemisorbed precursors. Barriers between these isomers are considered as activation energies of the formation of chemisorbed precursors. As stated above, the activation energies of the two cases are very similar, approximately 0.4 eV, and the chemisorbed species carry asimilar amount of charge. In other words, during the isomerization of the chemisorbed species, according to Figure 9 no significant charge transfer was observed between the metal slab and the chemisorbed species for either case. Thus, although the metal slabs still carry quite different charges (approximately +1.0 and 0 for the uncharged and charged systems), these charges do not affect much the energetics of the isomerization of the chemisorbed species. This may explain why the two models yield similar activation energies.

4. Summary

To investigate the electroreduction of O_2 over the Pt(111) surface, Car-Parrinello molecular dynamics simulations have been performed for the systems O_2 /Pt(111), $O_2+H^+(H_2O)_3$/Pt(111), and $O_2+H^+(H_2O)_3+e^-$/Pt(111). The study suggests the following points:

(a) At 350 K, a low-coverage O_2 (1/12 ML) is rapidly reduced with a rather low energy barrier via a one-end chemisorbed precursor (Pauling adsorption model).

(b) In the presence of $H^+(H_2O)_3$, a proton rapidly migrates to O_2, forming a H^+-O-O proton-transfer intermediate, which is followed by an electron transfer from the Pt slab. That process results in a chemisorbed precursor, $H-O-O-Pt_n$, in which the hydroxyl oxygen end is considerably further away from the surface than the O end.

(c) In the presence of an electron, the proton-intermediate H^+-O-O is also rapidly generated. However, the lifetime of the intermediate is longer and subsequent electron transfer is significantly delayed with respect to the case of the uncharged surface.

(d) In both the charged and uncharged surfaces, the calculated energy barrier for formation of $H-O-O-Pt_n$ is approximately 0.4 eV, while its decomposition does not show a clear barrier. Whether this is the overall OER rds needs further investigations of the complete reduction pathway.

(e) Based on these preliminary studies, the suggested mechanism for the first electron of OER is

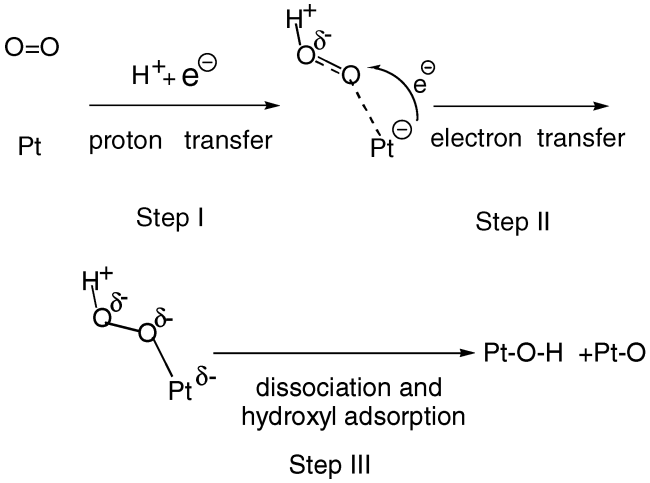

Acknowledgment. We acknowledge financial support from the National Science Foundation (CTS 9876065), Army Research Office (DAAD19-00-1-0087), and Department of Energy/Basic Energy Sciences, (DE-FG02-1ER15249). The use of computational facilities at the National Energy Research Scientific Computing Center, NERSC, is gratefully appreciated.

References and Notes

(1) Steele, B. C. H.; Heinzel, A. Materials for Fuel-Cell Technologies. *Nature* **2001**, *414*, 345.

(2) Marković, N. M.; Ross, P. N. Surface science studies of model fuel cell electrocatalysts. *Surf. Sci. Rep.* **2002**, *45*, 117.

(3) Gland, J. L.; Sexton, B. A.; Fisher, G. B. Oxygen interactions with the Pt(111) surface. *Surf. Sci.* **1980**, *95*, 587.

(4) Mainardi, D. S.; Calvo, S. R.; Jansen, A. P. J.; Lukkien, J. J.; Balbuena, P. B. Dynamic Monte Carlo Simulations of O_2 Adsorption and Reaction on Pt(111). *Chem. Phys. Lett.* **2003**, *382*, 553.

(5) Eichler, A.; Hafner, J. Molecular Precursors in the dissociative adsorption of O_2 on Pt(111). *Phys. Rev. Lett.* **1997**, *79*, 4481.

(6) Li, T.; Balbuena, P. B. Computational Studies of the Interactions of Oxygen with Platinum Clusters. *J. Phys. Chem. B* **2001**, *105*, 9943.

(7) Grimblot, J.; Luntz, A. C.; Fowler, D. E. Low-temperature adsorption of oxygen on Pt(111). *J. Electron Spectrosc. Relat. Phenom.* **1990**, *52*, 161.

(8) Steininger, H.; Lehwald, S.; Ibach, H. Adsorption of oxygen on platinum(111). *Surf. Sci.* **1982**, *123*, 1.

(9) Ranke, W.; Kuhr, H. J. Oxygen 2s spectroscopy. *Phys. Rev. B* **1989**, *39*, 1595.

(10) Puglia, C.; Nilsson, A.; Hernnaes, B.; Karis, O.; Bennich, P.; Martensson, N. Physisorbed, chemisorbed and dissociated O_2 on Pt(111) studied by different core level spectroscopy methods. *Surf. Sci.* **1995**, *342*, 119.

(11) Stoehr, J.; Gland, J. L.; Eberhardt, W.; Outka, D.; Madix, R. J.; Sette, F.; Koestner, R. J.; Doebler, U. Bonding and bond lengths of chemisorbed molecules from near-edge X-ray-absorption fine-structure studies. *Phys. Rev. Lett.* **1983**, *51*, 2414.

(12) Outka, D. A.; Stoehr, J.; Jark, W.; Stevens, P.; Solomon, J.; Madix, R. J. Orientation and bond length of molecular oxygen on silver(110) and platinum(111): a near-edge X-ray-absorption fine-structure study. *Phys. Rev. B* **1987**, *35*, 4119.

(13) Wurth, W.; Stoehr, J.; Feulner, P.; Pan, X.; Bauchspiess, K. R.; Baba, Y.; Hudel, E.; Rocker, G.; Menzel, D. Bonding, structure, and magnetism of physisorbed and chemisorbed O_2 on Pt(111). *Phys. Rev. Lett.* **1990**, *65*, 2426.

(14) Stipe, B. C.; Rezaei, M. A.; Ho, W.; Gao, S.; Persson, M.; Lundqvist, B. I. Single-molecule dissociation by tunneling electrons. *Phys. Rev. Lett.* **1997**, *78*, 4410.

(15) Stipe, B. C.; Rezaei, M. A.; Ho, W. Inducing and viewing the rotational motion of a single molecule. *Science* **1998**, *279*, 1907.

(16) Yeager, E. B. Electrocatalysts for O_2 reduction. *Electrochim. Acta* **1984**, *29*, 1527.

(17) Marković, N. M.; Gasteiger, H. A.; Grgur, B. N.; Ross, P. N. Oxygen reduction reaction on Pt(111): effects of bromide. *J. Electroanal. Chem.* **1999**, *467*, 157.

(18) Stamenkovic, V.; Marković, N. M.; Ross, P. N. *J. Electroanal. Chem.* **2000**, *500*, 44.

(19) Adzic, R. R.; Wang, J. X. Configuration and site of O_2 adsorption on the Pt(111) electrode surface. *J. Phys. Chem. B* **1998**, *102*, 8988.

(20) Bernardi, D. M.; Verbrugge, M. W. A mathematical model of the solid-polymer electrolyte fuel cell. *J. Electrochem. Soc.* **1992**, *139*, 2477.

(21) Greeley, J.; Mavrikakis, M. A first-principles study of methanol decomposition on Pt(111). *J. Am. Chem. Soc.* **2002**, *124*, 7193.

(22) Anderson, A. B.; Albu, T. V. Ab initio determination of reversible potentials and activation energies for outer-sphere oxygen reduction to water and the reverse oxidation reaction. *J. Am. Chem. Soc.* **1999**, *121*, 11855.

(23) Sidik, R. A.; Anderson, A. B. Density functional theory study of O_2 electroduction when bonded to a Pt dual site. *J. Electroanal. Chem.* **2002**, *528*, 69.

(24) Neurock, M. First-principles study of the role of solvent in the dissociation of water over a Pt−Ru alloy. *Phys. Rev. B* **2003**, *68*, Article: 075420.

(25) Car, R.; Parrinello, M. Unified Approach for Molecular Dynamics and Density-Functional Theory. *Phys. Rev. Lett.* **1985**, *55*, 2471.

(26) CPMD, 3.7.2 ed.; Copyright IBM Corp 1990−2003, Copyright MPI fuer Festkoerperforschung Stuttgart 1997−2001, 2003.

(27) Troullier, N.; Martins, J. L. Efficicient pseudopotentials for plane-wave calculations, *Phys. Rev. B* **1991**, *43*, 1993.

(28) Michaelides, A.; Hu, P. Catalytic water formation on platinum: A first-principles study, *J. Am. Chem. Soc.* **2001**, *123*, 4235.

(29) *Handbook of Chemistry and Physics*, 77th ed.; Lide, D. R., Ed.; CRC Press: Boca Raton, 1997.

(30) Hirshfeld, F. L. Bonded-atom fragments for describing molecular charge densities, *Theo. Chim. Acta* **1977**, *44*, 129.

(31) Frisch, M. J.; Trucks, G. W.; Schlegel, H. B.; Scuseria, G. E.; Robb, M. A.; Cheeseman, J. R.; Zakrzewski, V. G.; Montgomery, J. A., Jr.; Stratmann, R. E.; Burant, J. C.; Dapprich, S.; Millam, J. M.; Daniels, A. D.; Kudin, K. N.; Strain, M. C.; Farkas, O.; Tomasi, J.; Barone, V.; Cossi, M.; Cammi, R.; Mennucci, B.; Pomelli, C.; Adamo, C.; Clifford, S.; Ochterski, J.; Petersson, G. A.; Ayala, P. Y.; Cui, Q.; Morokuma, K.; Malick, D. K.; Rabuck, A. D.; Raghavachari, K.; Foresman, J. B.; Cioslowski, J.; Ortiz, J. V.; Stefanov, B. B.; Liu, G.; Liashenko, A.; Piskorz, P.; Komaromi, I.; Gomperts, R.; Martin, R. L.; Fox, D. J.; Keith, T.; Al-Laham, M. A.; Peng, C. Y.; Nanayakkara, A.; Gonzalez, C.; Challacombe, M.; Gill, P. M. W.; Johnson, B. G.; Chen, W.; Wong, M. W.; Andres, J. L.; Head-Gordon, M.; Replogle, E. S.; Pople, J. A. *Gaussian 98*, revision A.11; Gaussian, Inc.: Pittsburgh, PA, 1998.

(32) Balbuena, P. B.; Altomare, D.; Agapito, L. A.; Seminario, J. M. Adsorption of oxygen on Pt-based clusters alloyed with Co, Ni, and Cr. *J. Phys. Chem. B* **2003**, *107*, 13671.

(33) Xu, Y.; Mavrikakis, M. Adsorption and dissociation of O_2 on Ir-(111). *J. Chem. Phys.* **2002**, *116*, 10846.

(34) Campbell, C. T.; Ertl, G.; Kuipers, H.; Segner, J. A molecular beam study of the catalytic oxidation of carbon monoxide on a platinum(111) surface. *J. Chem. Phys.* **1980**, *73*, 5862.

(35) Yeo, Y. Y.; Vattuone, L.; King, D. A. Calorimetric heats for CO and oxygen adsorption and for the catalytic CO oxidation reaction on Pt-{111}. *J. Chem. Phys.* **1997**, *106*, 392.

(36) Chen, M.; Bates, S. P.; Santen, R. A. V.; Friend, C. M. The chemical nature of atomic oxygen adsorbed on Rh(111) and Pt(111): A density functional study. *J. Phys. Chem. B* **1997**, *101*, 10051.

(37) Jacob, T.; Muller, R. P.; Goddard, W. A. I. Chemisorption of Atomic Oxygen on Pt(111) from DFT Studies of Pt−Clusters. *J. Phys. Chem. B* **2003**, *107*, 9465.

(38) Marx, D.; Sprik, M.; Parrinello, M. Ab initio molecular dynamics of ion solvation. The case of Be^{2+} in water. *Chem. Phys. Lett.* **1997**, *273*, 360.

(39) Li, T.; Balbuena, P. B. Oxygen reduction on a platinum cluster. *Chem. Phys. Lett.* **2003**, *367*, 439.

(40) Michaelides, A.; Hu, P. A density functional theory study of hydroxyl and the intermediate in the water formation reaction on Pt. *J. Chem. Phys.* **2001**, *114*, 513.

(41) Shubina, T. E.; Koper, M. T. M. Quantum-chemical calculations of CO and OH interacting with bimetallic surfaces. *Electrochim. Acta* **2002**, *47*, 3621.